Max-Planck-Institut
für Meteorologie

REPORT No. 72

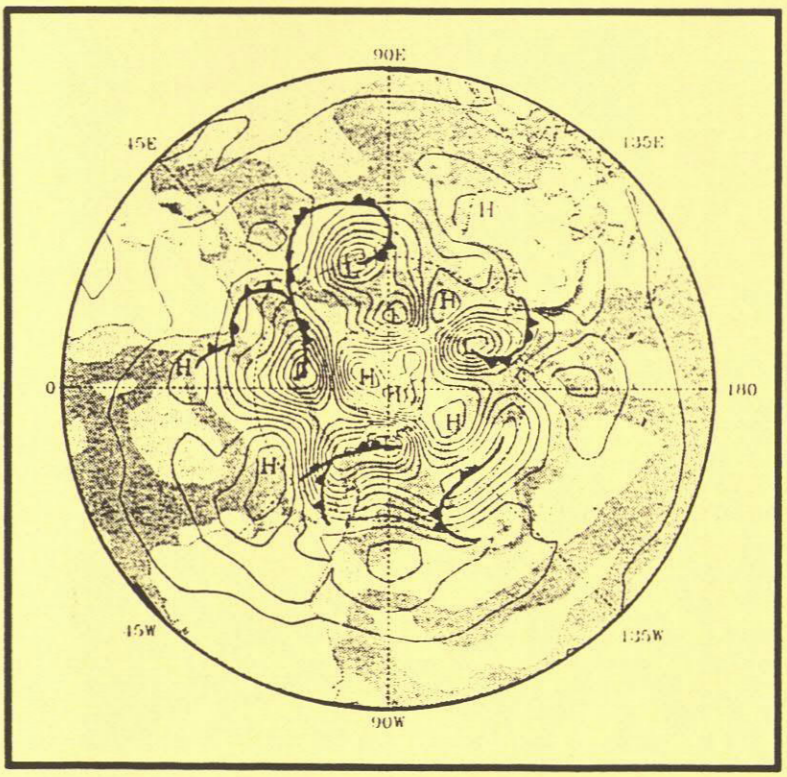

COUPLING AN OCEAN WAVE MODEL TO AN ATMOSPHERIC GENERAL CIRCULATION MODEL

by

SUSANNE L. WEBER • HANS von STORCH
PEDRO VITERBO • LIANA ZAMBRESKY

HAMBURG, SEPTEMBER 1991

AUTHORS:

SUSANNE L. WEBER
KONINKLIJK NEDERLANDS
METEOROLIGISCH INSTITUUT
POST BOX 201
3730 AE DE BILT
NETHERLANDS

HANS von STORCH
MAX-PLANCK-INSTITUT
FÜR METEOROLOGIE

PEDRO VITERBO
EUROPEAN CENTRE FOR
MEDIUM-RANGE WEATHER FORECASTS
SHINFIELD PARK
READING
BERKSHIRE RG 2 9 AX
GREAT BRITAIN

LIANA ZAMBRESKY
GKSS FORSCHUNGSZENTRUM
MAX-PLANCK-STR.
2054 GEESTHACHT
GERMANY

MAX-PLANCK-INSTITUT
FÜR METEOROLOGIE
BUNDESSTRASSE 55
D-2000 HAMBURG 13
F.R. GERMANY

Tel.: +49 (40) 4 11 73-0
Telex: 211092 mpime d
Telemail: MPI.METEOROLOGY
Telefax: +49 (40) 4 11 73-298

REPb72

COUPLING AN OCEAN WAVE MODEL TO AN ATMOSPHERIC GENERAL CIRCULATION MODEL

Susanne L. Weber
Royal Netherlands Meteorological Institute
De Bilt, The Netherlands

Hans von Storch
Max-Planck-Institute for Meteorology, Hamburg, Germany

Pedro Viterbo
European Centre for Medium-Range Weather Forecasts
Reading, Great Britain

Liana Zambresky
GKSS Research Centre
Geesthacht, Germany

ISSN 0937–1060

Abstract

A coupled model, consisting of an ocean wave model and an atmospheric general circulation model (AGCM), is integrated under permanent-July conditions. The wave model is forced by the AGCM wind stress, whereas the effect of the ocean waves is transferred to the AGCM in terms of modified surface fluxes of momentum and heat. Two aspects of the coupled model are investigated: first, whether the ocean wave fields are realistic and second, whether the atmospheric circulation is modified by the surface fluxes induced by the spatially and temporally varying wave field.

The coupled model generates waves with mean wave heights of 1 - 2 m in the Northern Hemisphere and in the tropics, and of more than 3 m in the Southern Hemisphere storm track. These compare favorably with observational data. Young wind sea, which is associated with enhanced surface fluxes, is generated in the storm track in the Southern Hemisphere, in the Northern Hemisphere subtropics and in the Arabian Sea.

The atmospheric circulation in the coupled experiment differs only in the Southern Ocean storm belt from the circulation in a control experiment without the wave model. The time-mean meridional gradient of 500 hPa geopotential height is steepened. The high-frequency variance, representative of baroclinic disturbances, is shifted poleward and is intensified at high latitudes.

Young wind sea is generated mostly in the equatorward "frontal" area of a cyclone. Our "storm-wave interaction" hypothesis proposes that the inhomogeneous distribution of surface roughness below a cyclone accelerates the poleward movement of cyclones. At the same time the cyclones live longer, or they become more frequent. Thus, the process of generating ocean waves is likely important for weather forecasting.

1. INTRODUCTION

Wind waves are a significant feature of the interface between the atmosphere and the ocean. Even with a light breeze small ripples are present on the ocean surface. Storms over the open ocean easily generate waves with wave heights of 5-10 m. The momentum and heat fluxes through the interface are modified by the presence of waves on the interface. Ocean waves are therefore of interest for climate studies, both for modeling of the atmosphere and the ocean separately and for modeling of the coupled ocean-atmosphere system (Hasselmann, 1990).

A theory of coupled wind-wave growth is given by Janssen (1989): waves are generated when wind is blowing over the ocean surface, so that the air flow feels an additional stress due to the momentum flux to the wave field. The momentum which is transferred to the growing waves is called the wave-induced stress. It is large in the initial stage of wave growth, i.e. immediately after an increase in the wind speed or a change in the wind direction. Observations have confirmed that the surface stress is enhanced for young wind sea (Maat et al., 1991). Therefore, the roughness length of the sea surface should be a function of the wave-induced stress.

A global increase in the surface roughness seems to have almost no effect on the atmospheric general circulation, except for slightly slowing down the boundary layer flow (Sausen, personal communication). On the other hand, Ulbrich et al. (1991) found that a strongly increased surface roughness in the southern ocean storm track produces a significant modification of the atmospheric circulation.

In the present study detailed models of the atmospheric circulation and of the ocean wave field are coupled together. With this coupled model we test whether a realistic wave field is induced by the atmospheric general circulation model (AGCM) and whether the atmospheric circulation responds to the varying ocean roughness. The atmospheric GCM and the wave model are briefly described in section 2, with emphasis on the coupling through the sea surface roughness. The performance of the coupled model is discussed in section 3: the simulated wave fields are compared with semi-operational wave data from the European Centre for Medium range Weather Forecasts (ECMWF), and the atmospheric fields are compared with fields obtained in an uncoupled control run. We conclude with a summary and a discussion of the results in section 4.

An interesting by-product of the present study refers to the sensitivity of the GCM atmospheric flow to an imposed minimum value of the sea surface roughness. This is discussed in the Appendix.

2. The Coupled Model

The coupled model consists of the WAM wave model (WAMDIG, 1989) and the ECHAM2 atmospheric GCM (Roeckner et al., 1989). It is integrated under fixed-July conditions, so that the incoming solar radiation and the sea-surface temperature do not vary. A fixed-month mode was chosen to get time series which are long and statistically stationary, so that a meaningful statistical analysis can be performed.

An integration over a longer time and in the annual-cycle mode would be preferable. Because of limited computer time this was not possible: a simulation of 30 days with the coupled WAM-ECHAM2 model requires 2.5 hours CPU time on a Cray 2, compared to only 0.5 hours for ECHAM2 alone.

In a simulation with permanent July conditions the Northern Hemisphere continents experience an eternal summer. Less and less radiative energy is needed for evaporation and the atmosphere warms slowly. Thus, the permanent-July mode causes a trend in the model (Zwiers and Boer, 1987), which is mostly confined to the Northern Hemisphere. The trends cancel each other in the difference fields of the experiment with WAM and the experiment with WAM.

2.1 The ocean wave model

The wave model (WAMDIG, 1989) computes the local change of the wave spectrum on a regular $3^\circ \times 3^\circ$ grid, extending from 63° S to 81° N. It is forced by the stress exerted by the wind on the ocean surface. The wave model describes the generation of waves by the wind, the dissipation by white capping, the transfer of energy within the wave spectrum by the resonant four-wave interactions and the advection of energy by wave propagation. As waves grow the total energy of the wave field increases while the energy-containing range of the spectrum shifts to lower frequencies, until the wave field and the wind are in equilibrium.

A characteristic parameter of the wave field, which is commonly used, is the *significant wave height* H_s. This quantity is defined as $H_s = 4\sqrt{E}$, with E the integral over all spectral components of the wave variance spectrum.

Global maps of the wave height directly derived from observations do not exist. We verify our results with forecasts prepared on a semi-operational

basis at the ECMWF. These forecasts were obtained by forcing the WAM model with analyzed winds from the operational ECMWF weather forecast model. The forecasted wave heights have been verified against various data (buoys, ship records, satellite data), most extensively by Zambresky (1989) and Romeiser (1990). From a comparison for the year 1988 with moored buoy data Zambresky finds that the wave height is predicted with a high degree of accuracy, even though the model tends to underestimate extreme waves. A verification against GEOSAT data for the same year by Romeiser shows a small negative bias in the monthly mean wave height; in the Southern Hemisphere the "observed" ECMWF wave height underestimates the real wave height by 20% at most in July, primarily because of too weak forcing.

2.2 The atmospheric general circulation model

The atmospheric GCM is the Hamburg version of the ECMWF spectral model with T21 resolution, named ECHAM2. A T21 spectral resolution is comparable to a $5.6^\circ \times 5.6^\circ$ horizontal grid. The model has been designed for climate studies (Roeckner et al., 1989).

In the standard ECHAM2, with no wave model coupled to it, the roughness length z_0 is given over open sea by the Charnock formula (Charnock, 1955):

$$z_0 = \alpha \frac{\tau}{g\rho} \qquad (1)$$

Here τ is the magnitude of the turbulent stress, g is the gravitational constant, ρ is the density of air and α is a tunable proportionality constant, which is set to $\alpha = 0.018$. The Charnock formula (1) is modified by a minimum condition: in the case of laminar flow (low wind speeds) z_0 is set to 0.15 mm (see also the Appendix).

The drag coefficient at height z for the neutrally stratified atmospheric boundary layer is given by:

$$c_D(z) = \{0.4/\ln (z/z_0)\}^2 \qquad (2)$$

Because $\tau = \rho\, c_D\, U^2$, (1) and (2) implicitly define c_D and z_0 as functions of the wind speed U at height z. The drag coefficient increases with increasing wind speed. For the neutral atmosphere (2) also gives the exchange coefficient for the sensible and latent heat fluxes. In nonneutral cases the exchange coefficients for momentum and heat are modified by a factor which depends on

the atmospheric stability. For the unstable boundary layer the coefficients are enhanced, whereas for the stable boundary layer they are reduced.

2.3 The coupling of the two models

Waves grow on the ocean surface due to shear-flow instability of the wind (Miles, 1957). At the "critical height", where the wind equals the wave phase velocity, resonance occurs between the surface waves and the air flow. The small perturbations in the air flow, which are associated with the wave motion, act as a stress. This additional stress is called the wave-induced stress. In this respect air flow over water differs from flow over a rigid surface where there is only the turbulent stress. Miles assumed that the wave-induced stress is small compared to the total stress, so that the air flow and wave motion can be considered as uncoupled.

Extending Miles' theory, Janssen (1989) took into account the interaction between the turbulent atmospheric boundary layer and the waves generated by it. The wave-induced stress is large in the initial stages of wave growth, when *young* wind sea prevails in the wave field. This occurs immediately after an increase in the wind speed or a change in the wind direction. Thus the atmospheric boundary layer is transferring considerably more momentum into the ocean when the air flow is over *young* wind-sea, than when it is over *old* wind sea (with identical significant wave height). Young wind sea ages quickly and, if the situation is stationary, the coupling is strong only during 6-12 hours (Janssen et al., 1989).

The wave-induced stress is defined as the integral over all spectral components of the atmospheric momentum flux into the wave field (Janssen, 1989). It is primarily determined by the high-frequency waves, which are generated quasi-instantaneously by the local wind. Longer waves, which may have been generated by earlier winds elsewhere, contribute less to the wave-induced stress. However, longer waves influence the energy balance of the shorter wave components and thereby they also contribute to the wave-induced stress.

The coupling scheme used in the present experiment is based on Janssen's theory. If τ denotes the total (turbulent *and* wave-induced) stress and τ_w the wave-induced stress, then the roughness length z_0 is:

$$z_0 = \beta \frac{\tau}{g\rho(1-\tau_w/\tau)^m} \qquad (3)$$

In our model the parameters are set to m = 0.8 and β = 0.016. The fetch and the duration of the wind enter in (3) through the factor τ_w/τ, which is a function of the wave age. For *young* wind sea, which occurs for short fetches and short duration, $\tau_w/\tau \geq 0.4$. For *old* wind sea, with $\tau_w/\tau \approx 0.1$, (3) reduces to (1).

The discretization of the coupling scheme is as follows. At the end of every time step (40 min) the surface stress is computed from the lowest-level wind, using the drag coefficient of the previous time step. The atmospheric model communicates the stress to the wave model and WAM then performs the same time step. The resulting wave-induced stress is passed on to ECHAM2. The turbulent stress, which corresponds to the lowest-level wind under neutral conditions, and the wave-induced stress are added. The roughness length is calculated from (3) and the drag coefficient is updated according to (2), taking the atmospheric stratification into account.

Molecular viscosity is not considered in the theory of coupled wave growth, so that the coupling scheme does not apply if the boundary layer is viscous. By accident, the minimum roughness value of 0.15 mm was replaced by an extremely low minimum of 0.0001 mm in the WAM-ECHAM2 model. For the sake of consistency the control run, performed with ECHAM2 alone, was also conducted with this unrealistic low value. Instances of low wind speeds are not considered in the analysis of the results, as the physics of the coupled model is not realistic for viscous flow. We will come back to the question of the minimum roughness value in Section 3.2 and in the Appendix, where the sensitivity of the GCM to the imposed minimum z_0 is discussed.

Wave growth affects the momentum flux at the surface. It is not clear from the theory of coupled wind-wave growth whether the heat fluxes are also modified. Observations indicate that ocean waves enhance the heat fluxes also, although not as strongly as the momentum fluxes (DeCosmo, 1991). In the present experiment we compute the transfer coefficients for the sensible and latent heat fluxes from the modified roughness length (3).

3. RESULTS

The coupled WAM-ECHAM2 model has been integrated in the permanent-July mode for 390 days. The wave fields reach a quasi-stationary state in less than 30 days. The first 30 days are therefore disregarded in the following analysis. The time-mean over the last 360 days is denoted by an overbar.

First we do a case study of a randomly chosen set of six consecutive 12-hour periods from the model (Subsection 3.1). Then, time-mean fields of the significant wave height, the wave-induced stress and the sea surface roughness (Subsection 3.2) as well as the atmospheric response to the modified sea surface conditions are discussed (Subsection 3.3).

3.1 A Case Study

Maps of the 12-hourly mean sea level pressure are shown in Fig. 1 together with 12-hourly mean values of the stress ratio τ_w/τ for six consecutive 12-hour periods (days 141 - 143). The stress ratio denotes the strength of the coupling between the waves and the atmospheric flow. In the diagrams "fronts" have been placed subjectively, even though small-scale features like fronts are not resolved by our coarse resolution GCM. The "fronts" are connected with the position of strongest horizontal temperature gradients at the 850 hPa level. In Fig. 2 the significant wave height and the mean wave direction are shown for the same six time periods.

The stress ratio field (Fig. 1) is spatially and temporally highly variable. The distribution under an individual cyclone is inhomogeneous: stress ratio maxima, which represent young wind sea, occur on the equatorward "frontal" side of the cyclone. A good example of such an inhomogeneous distribution is the low which develops at 65° E, 45° S. In this case a considerable coupling persists beyond the mature stage of the storm. In other cases the waves age at the same time as the storm itself, so that at the end

---

Figure 1

The sea level pressure and the stress ratio τ_w/τ for 6 consecutive 12-hour periods from the coupled wave-atmosphere model in permanent-July mode, beginning with day 141 (0-12 UTC) and ending with day 143 (12-24 UTC). All values are 12-hourly means.

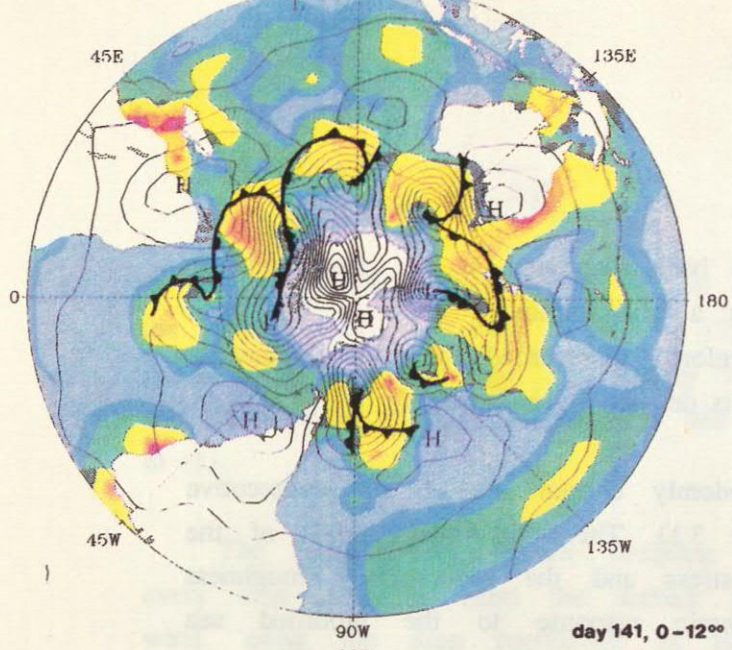

day 141, 0–12°°

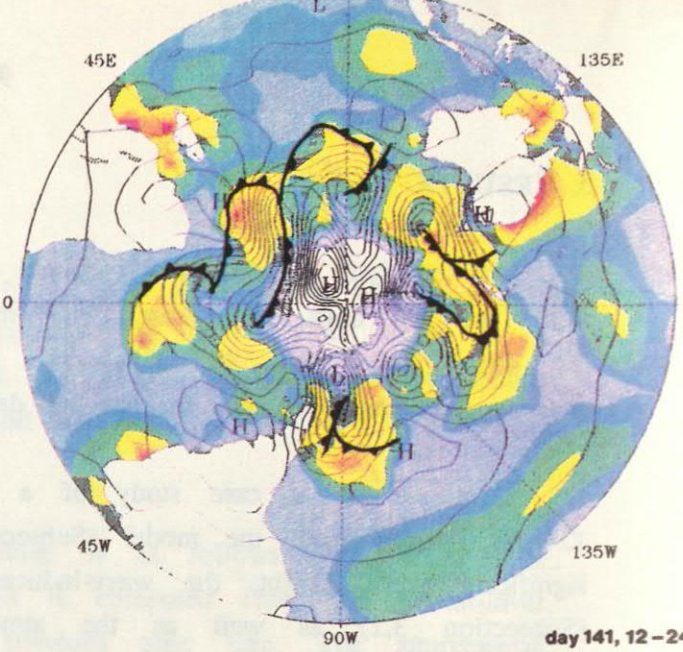

day 141, 12–24°°

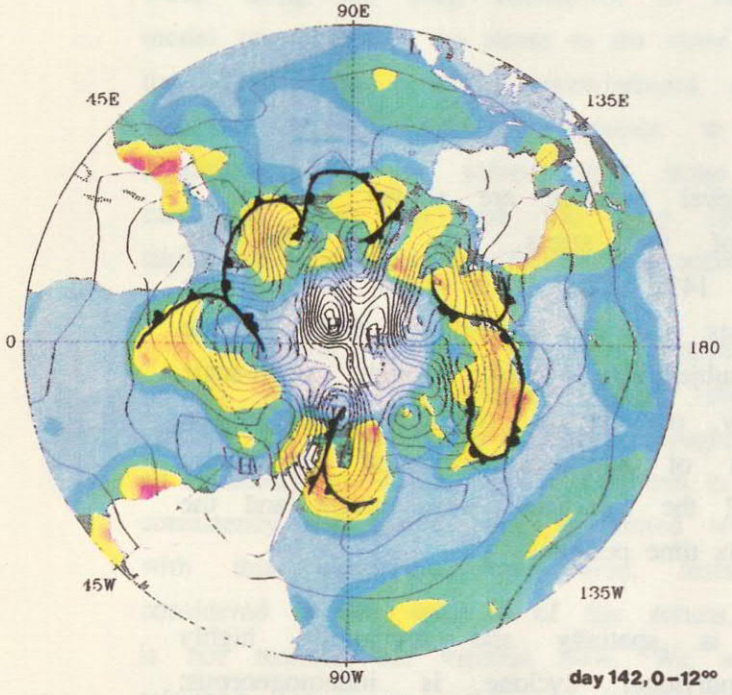

day 142, 0–12°°

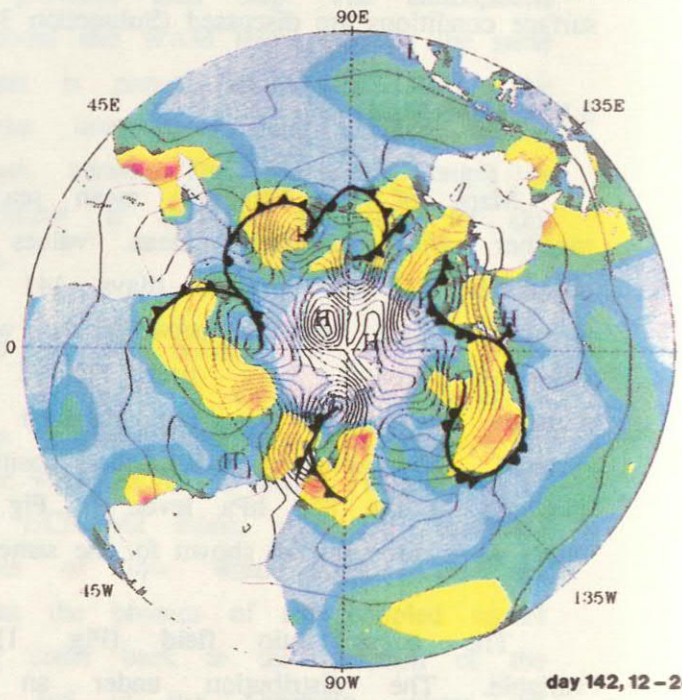

day 142, 12–24°°

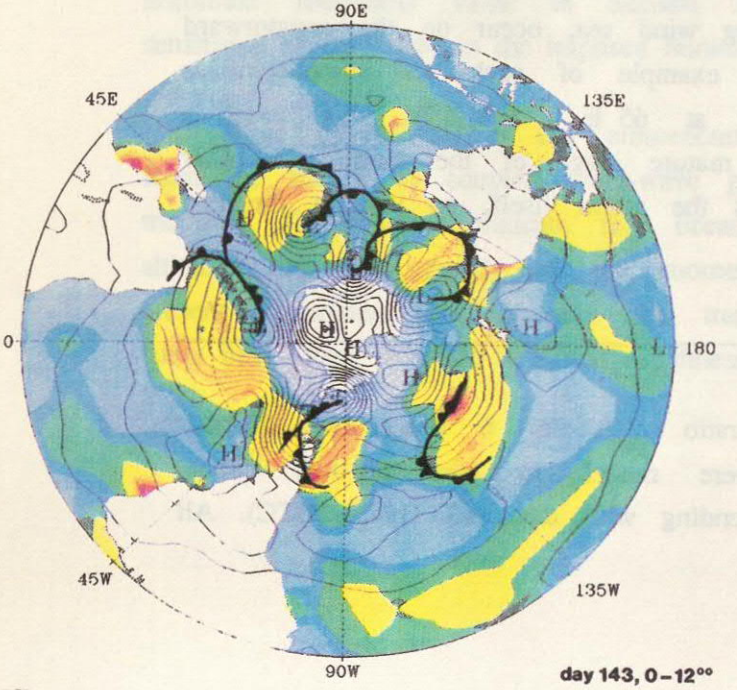

day 143, 0–12°°

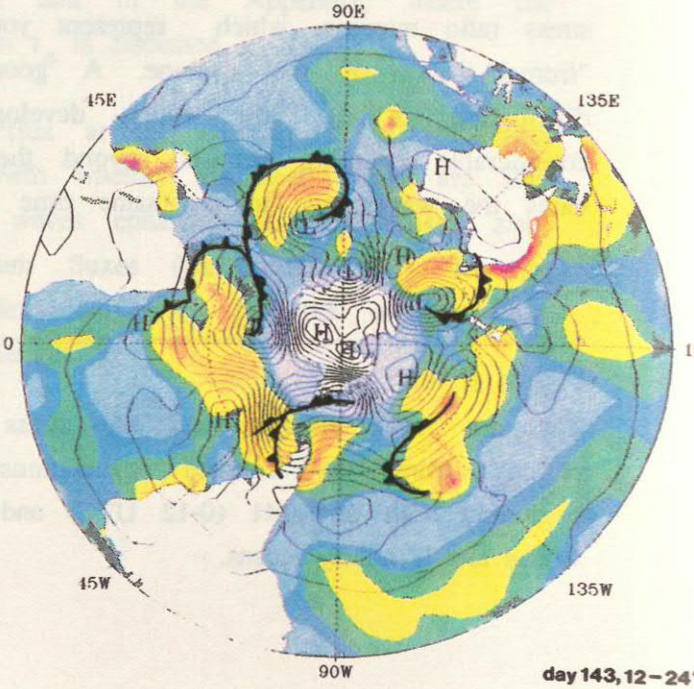

day 143, 12–24°°

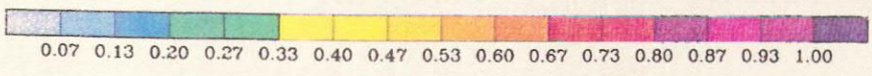

of a storm's life cycle the underlying wave field is old. An example is the storm which travels southward at 90°E. High stress ratios are also found westward off the continents, where the fetch is limited in a westerly flow.

The wave height fields (Fig. 2) reflect the surface winds, with wave height maxima near lows. The mean wave direction is considerably less variable than the wind direction. In midlatitudes the waves propagate in the climatological mean wind direction, rather than the direction of the high-frequency (daily) wind. Wave propagation out of the storm track is clearly reflected by the mean wave direction in the subtropics and tropics and in high latitudes, where the wave direction and the wind direction are mostly perpendicular.

We clarify some of the features discussed above in Fig. 3, where time series are shown of the 10-m wind, τ_w/τ and H_S at a north-south section at 51°E for the same time period as in Figs. 1 and 2. On the first day a high-pressure system is prevailing at 60°S with a ridge extending equatorward (Fig. 1). At the same time a cyclone is approaching from the west. The passage of the cyclone is reflected by the clockwise rotating wind north of 48°S, and by the anti-clockwise rotation south of 48°S. On the equatorward side of the cyclone a "front" appears (37°S, 42°S), with strong surface winds with a maximum wind speed of 24 m/s. Here energetic young wind sea with a wave height of 7-8 m and 12-hourly mean τ_w/τ = 0.5 is present. Equatorward of the "front" (31°S) and poleward (48°S, 53°S and 59°S) of the cyclone center the winds are weaker and the wave height and τ_w/τ are much lower.

Figure 2

The significant wave height and the mean wave direction for 6 consecutive 12-hour periods from the coupled wave-atmosphere model in permanent-July mode, beginning with day 141 (12 UTC) and ending with day 143 (24 UTC). All values are instantaneous.

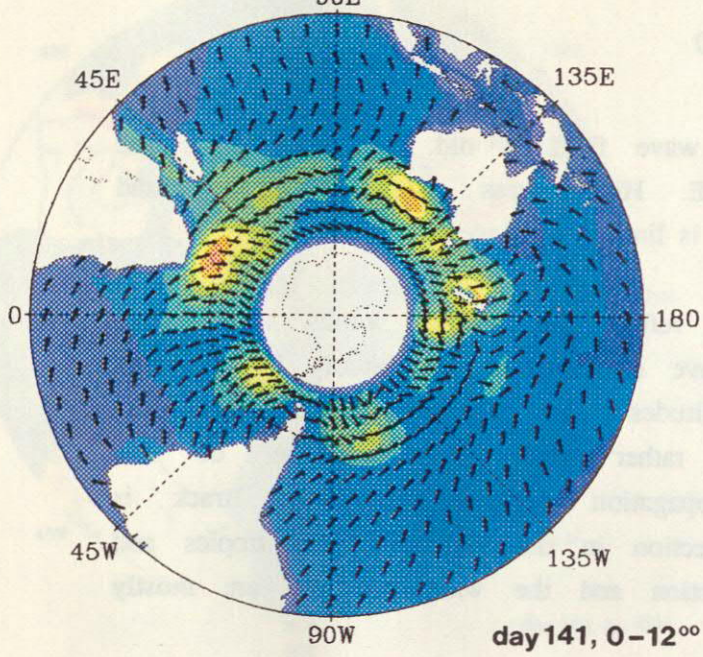

day 141, 0–12°°

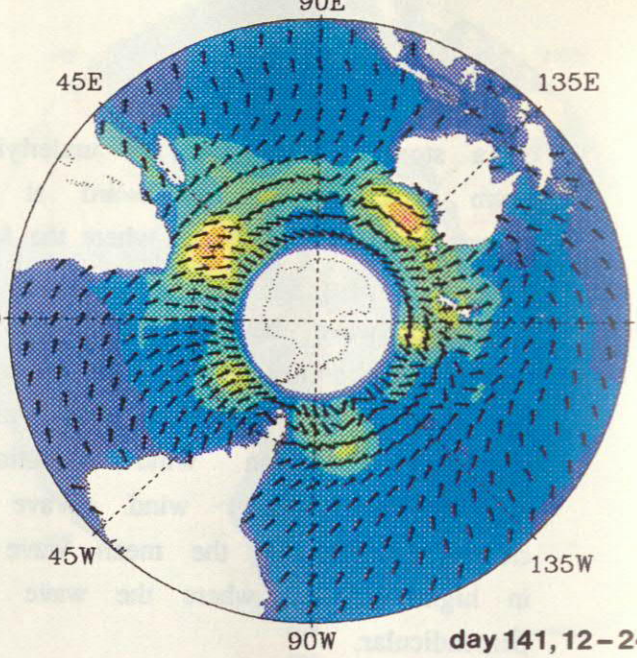

day 141, 12–24°°

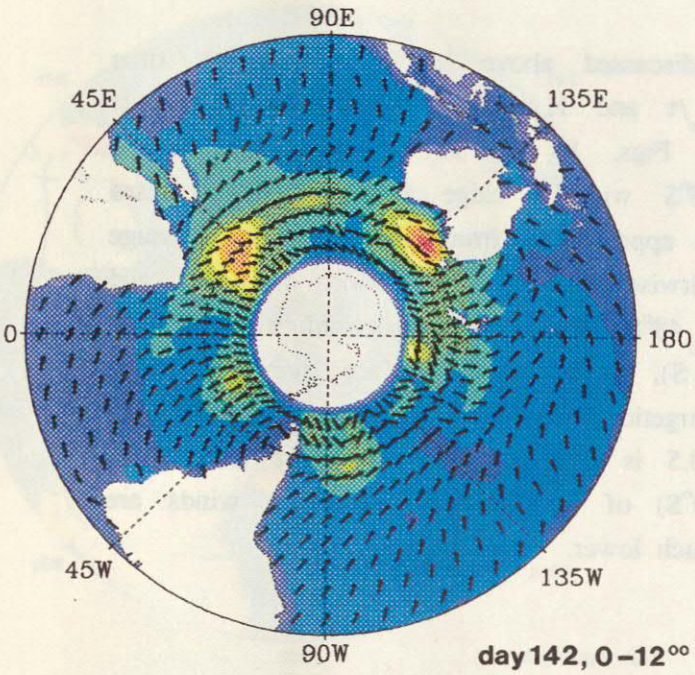

day 142, 0–12°°

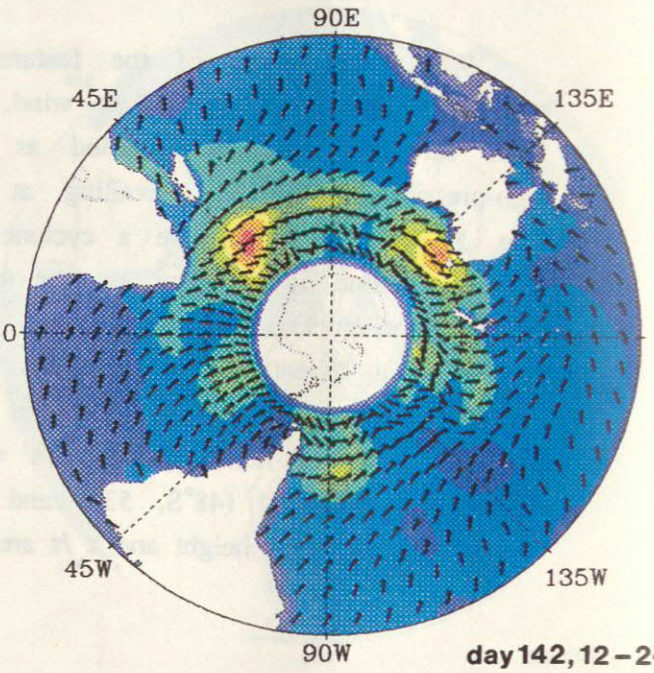

day 142, 12–24°°

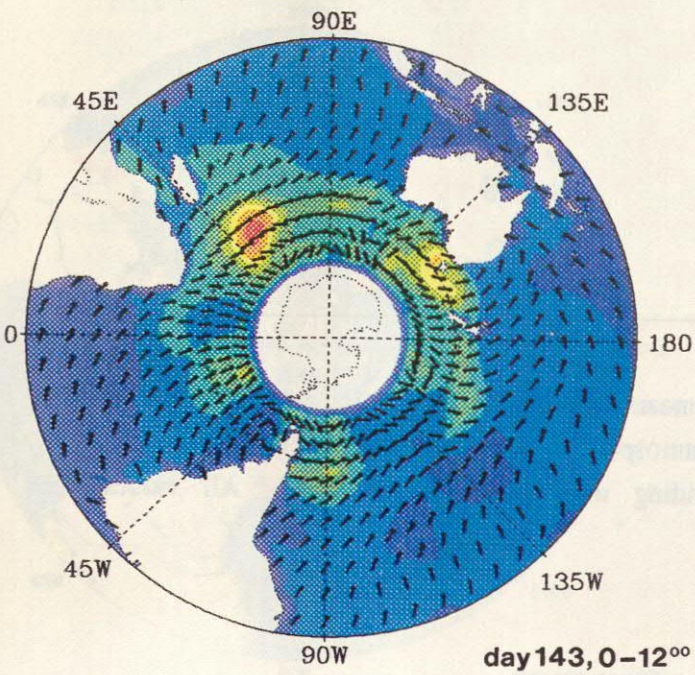

day 143, 0–12°°

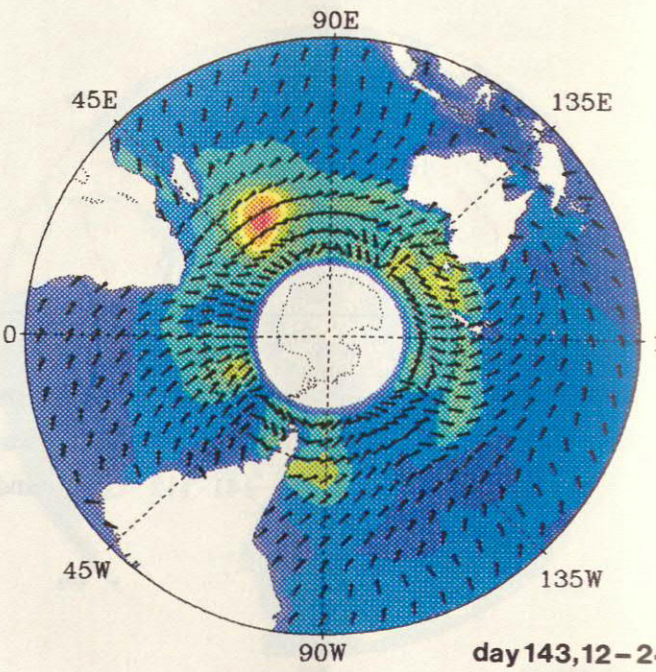

day 143, 12–24°°

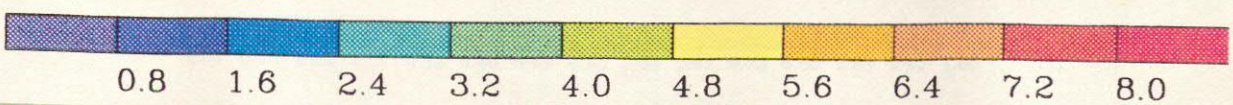

Figure 3

Time series of the magnitude of the 10 m-wind, the stress ratio τ_w/τ and the wave height at six grid points along a north-south section at 51 E for six consecutive time intervals, beginning with day 141 (0-12 UTC) and ending with day 143 (12-24 UTC). Wind and wave direction are indicated, with arrows pointing up indicating north. The atmospheric data are 12-hourly means; the wave data are instantaneous. The time-interval coincides with that in Figs. 1 and 2.

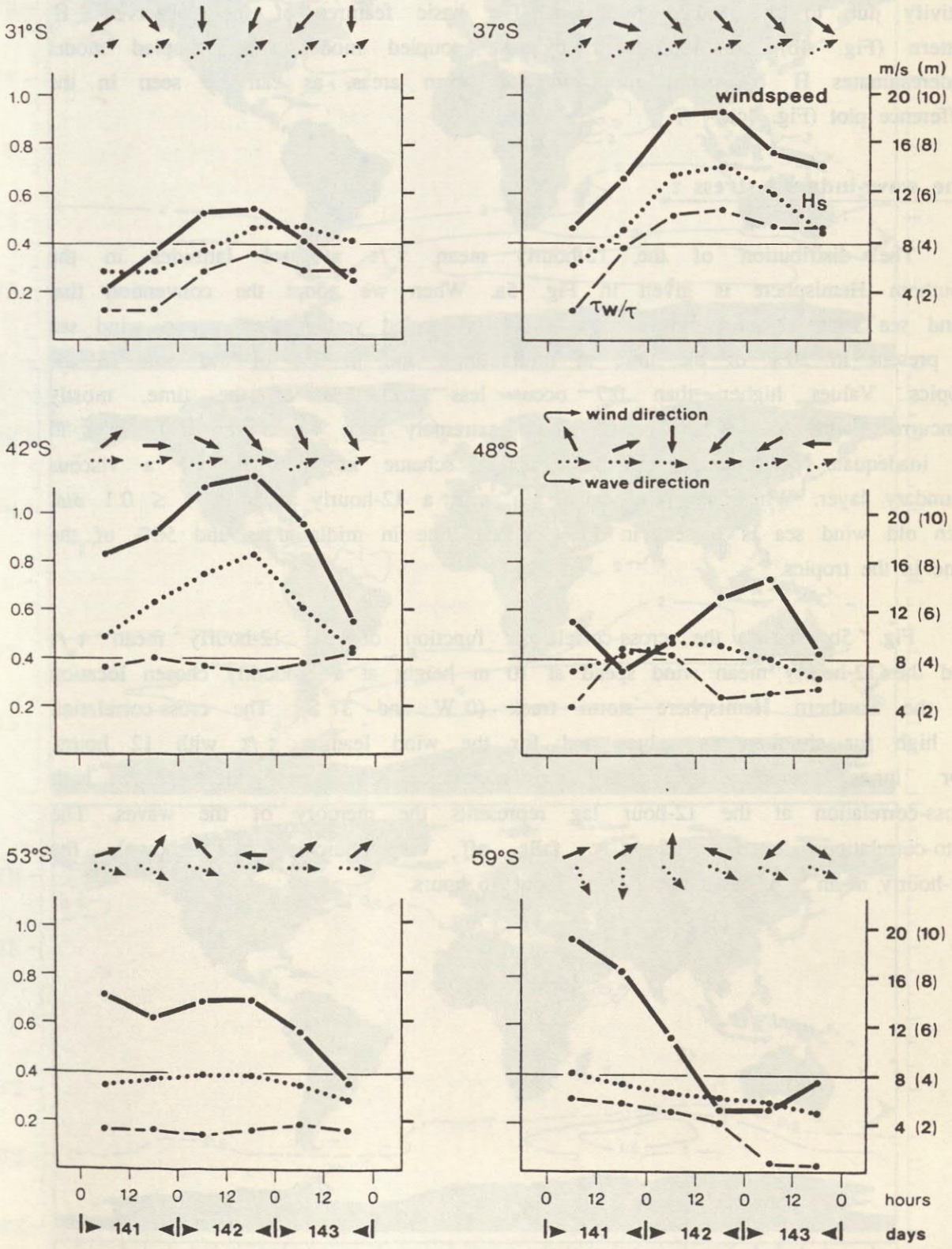

3.2 Climatology of the coupled model

The significant wave-height H_s

The mean significant wave height H_s in the coupled WAM-ECHAM2 experiment is 3 m in the Southern Ocean storm track (Fig. 4a). An exception is the southwest Pacific, where the waves and winds are less energetic. The wave height is 1-2 m north of 20° S, except in the Arabian Sea where there is storm activity due to the Indian Monsoon. The basic features of the "observed" H_s pattern (Fig. 4b) are reproduced by the coupled model. The coupled model underestimates H_s by about 1 m in the storm areas, as can be seen in the difference plot (Fig. 4c).

The wave-induced stress τ_w

The distribution of the 12-hourly mean τ_w/τ at two latitudes in the Southern Hemisphere is given in Fig. 5a. When we adopt the convention that wind sea with 12-hourly mean $\tau_w/\tau \geq 0.4$ is labeled *young*, then young wind sea is present in 20% of the time at midlatitudes and in 5% of the time in the tropics. Values higher than 0.7 occur less than 1% of the time, mostly concurrent with low wind speeds. These extremely high values might be due to an inadequate performance of the coupling scheme in the case of a viscous boundary layer. When we label wind sea with a 12-hourly mean $\tau_w/\tau \leq 0.1$ *old*, then old wind sea is present in 15% of the time in midlatitudes and 50% of the time in the tropics.

Fig. 5b shows the cross-correlation function of the 12-hourly mean τ_w/τ and the 12-hourly mean wind speed at 10 m height at a randomly chosen location in the Southern Hemisphere storm track (0° W and 37° S). The cross-correlation is high for simultaneous values and for the wind leading τ_w/τ with 12 hours. For longer time lags, the cross-correlation is negligible. The high cross-correlation at the 12-hour lag represents the memory of the waves. The auto-correlation function of τ_w/τ falls off very quickly (not shown); the 12-hourly mean τ_w/τ has a memory of about 16 hours.

Figure 4

The July-mean significant wave height $\bar{H}_s$ (in m):

a) as simulated by the coupled wave-atmosphere model (360-day mean).

b) as forecasted by ECMWF from analysed winds (mean over July 1987, 1988, 1989 and 1990).

c) difference between a) and b).

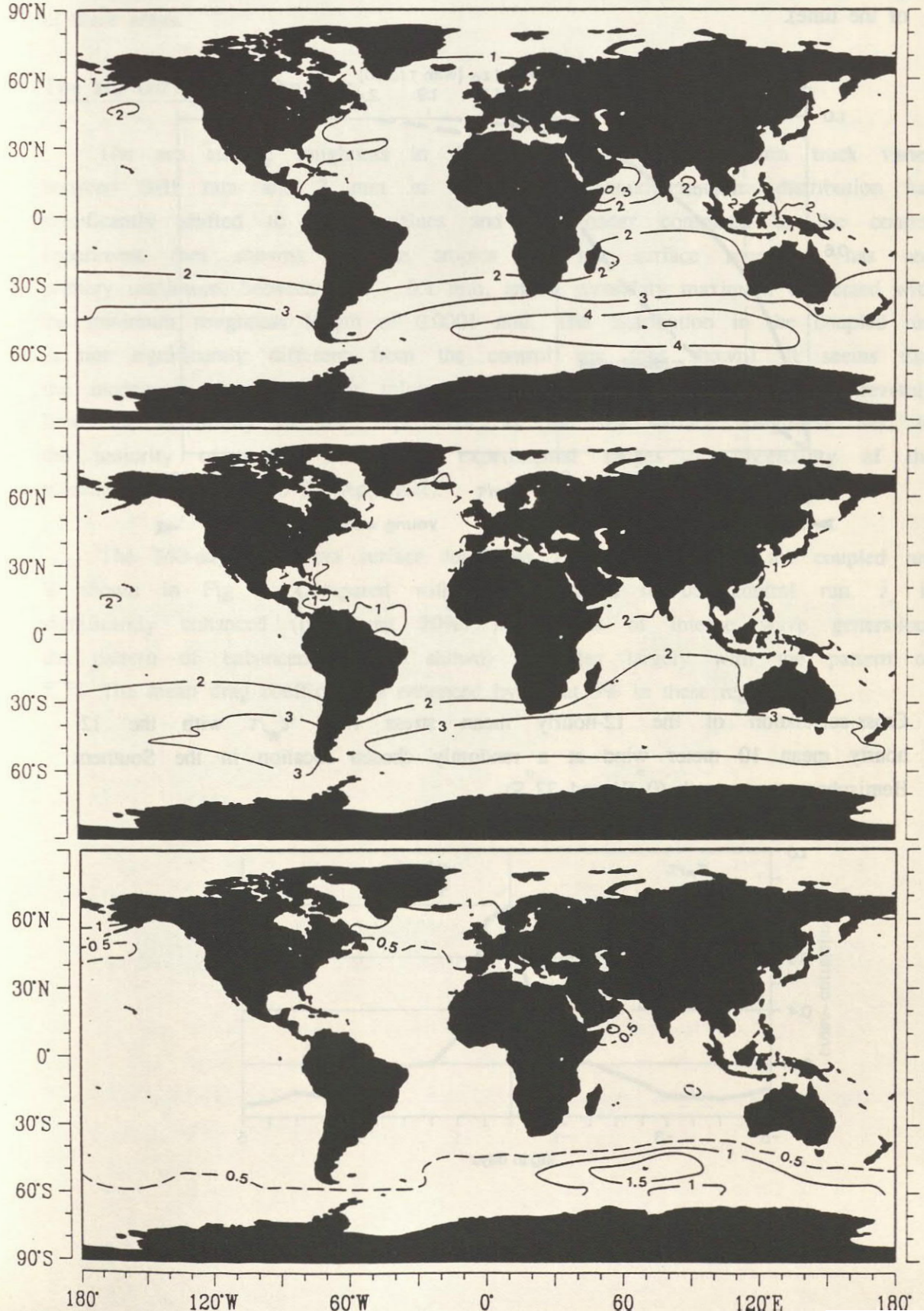

Figure 5

a) The distribution function of the 12-hourly mean stress ratio τ_w/τ at a tropical latitude (3° S) and at a storm track latitude (42° S) in the Southern Hemisphere. The coupling between the wave model and the AGCM can be neglected in the tropics (where low stress ratios prevail) and is weak in the mean in midlatitudes (where high stress ratios are present in 20% of the time).

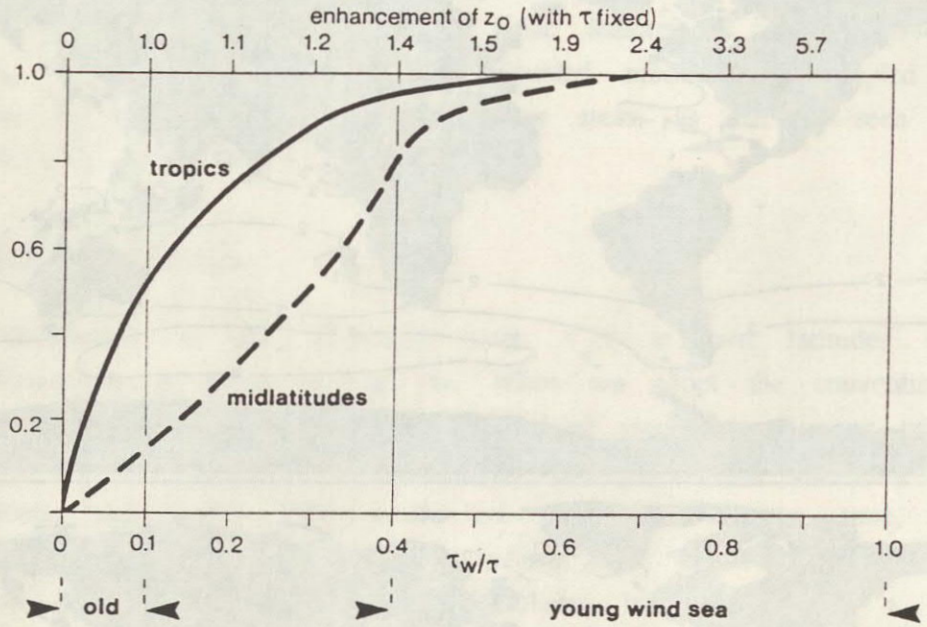

b) Cross-correlation of the 12-hourly mean stress ratio τ_w/τ with the 12-hourly mean 10 meter wind at a randomly chosen location in the Southern Hemisphere storm track (0° W and 37° S).

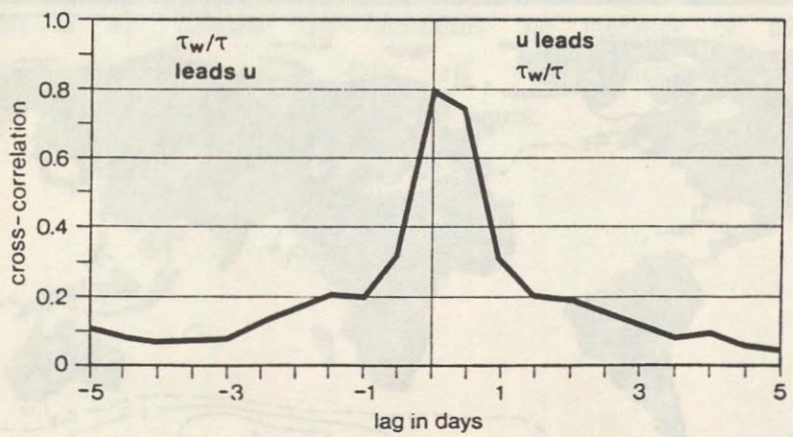

Finally we consider the 360-day mean ratio $\overline{\tau_w/\tau}$ (Fig. 6). Over most of the ocean, and in particular over most of the tropical ocean, old wind sea prevails. Larger values ($\overline{\tau_w/\tau}$ = 0.2-0.3) are found in the Southern Hemisphere storm track, in the Arabian Sea and at some spots in the Northern Hemisphere. Apparently, these are the regions where young wind sea is generally present in the coupled system. Note that the mean wave height (Fig. 4a) is small in part of these areas.

The sea surface roughness z_0

The sea surface roughness in the Southern Hemisphere storm track varies between 0.01 mm and 3 mm in the coupled experiment; the distribution has significantly shifted to larger values and is broader compared to the control experiment (not shown). In the tropics the sea surface roughness has one primary maximum, between 0.01 - 0.1 mm, and a secondary maximum connected with the minimum roughness length of 0.0001 mm. The distribution in the coupled run is not significantly different from the control run (not shown). It seems that the inadequate choice of the minimum z_0 in our experiment does not severely limit the credibility of the experiment, as the sea surface roughness lies, in the majority of cases, within the experimental ranges of uncertainty of the minimum value (see also the Appendix).

The 360-day mean sea surface roughness $\bar{z}_0$ as simulated in the coupled run is shown in Fig 7. Compared with the roughness in the control run, $\bar{z}_0$ is significantly enhanced (by about 20%) in regions of intense wave generation: the pattern of enhancement (not shown) coincides largely with the pattern of $\overline{\tau_w/\tau}$. The mean drag coefficient is enhanced by about 5% in these regions.

Figure 6
The 360-day mean ratio $\overline{\tau_w/\tau}$ of the wave-induced stress τ_w to the total stress τ in the coupled WAM-ECHAM2 experiment. Long-term mean values $\overline{\tau_w/\tau} \leq 0.1$ indicate that the wave field consists almost always of old waves. In areas with $\overline{\tau_w/\tau}$ = 0.2-0.3 young wind sea is relatively frequent present.

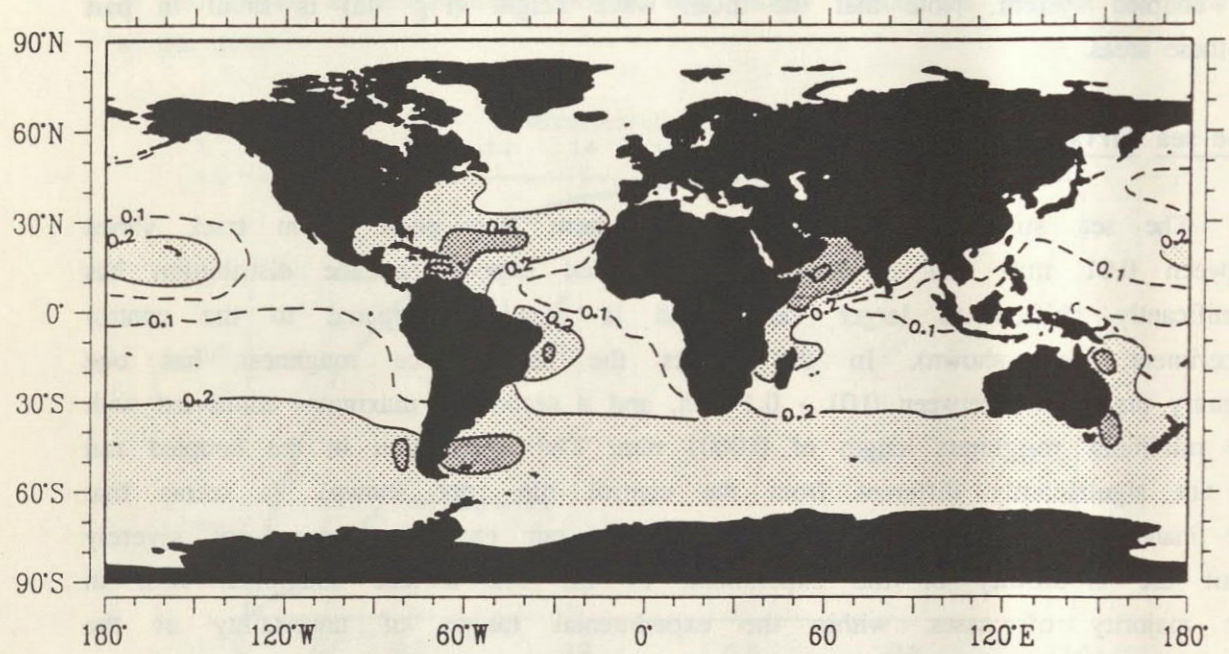

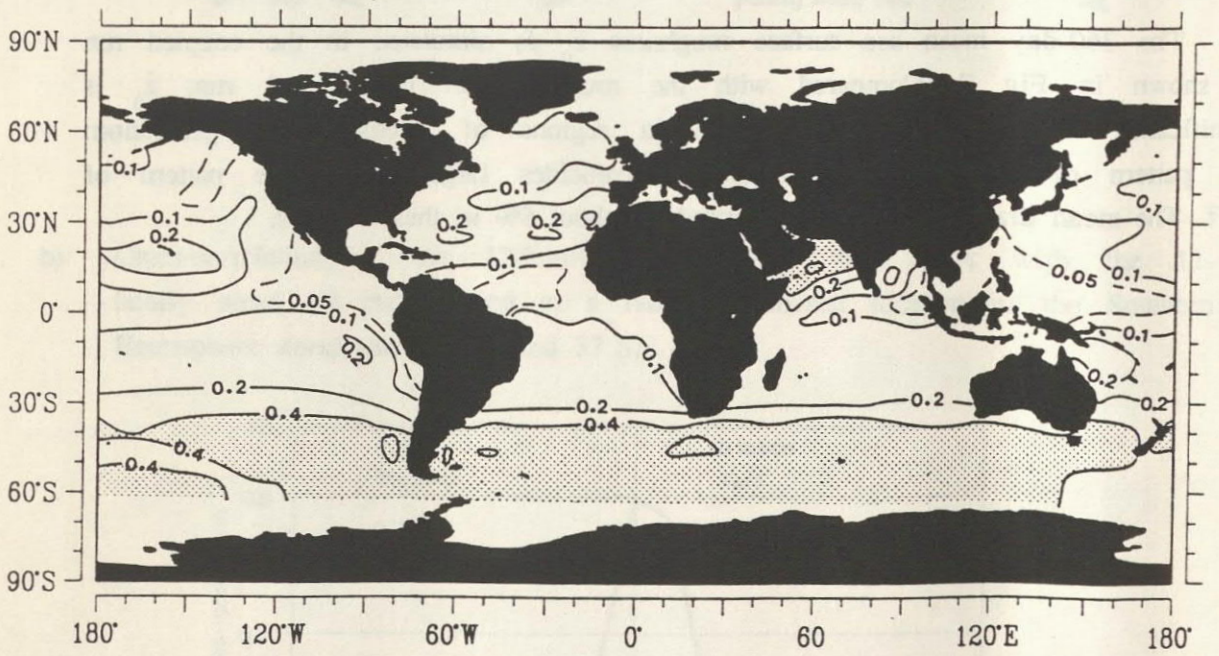

Figure 7
The 360-day mean sea surface roughness $\bar{z}_0$ (in mm) in the coupled WAM-ECHAM2 experiment.

3.3 Zonally averaged atmospheric parameters

The statistical stability of the atmospheric response to the space-time variable surface roughness is quantified by the locally estimated level of recurrence p (Storch and Zwiers, 1988). The larger the number p is, the smaller is the overlap between the two experiments. The level of recurrence p is defined in such a way that p is large (small) when a positive (negative) anomaly at a given location has a high change to reoccur in any individual 30-day mean field. Note that the estimated level of recurrence does not imply any assessment of the risk to reject the null-hypothesis of a zero signal. We prefer the recurrence analysis over the conventional hypothesis test because the outcome of the latter is sensitive to the number of independent samples, whereas the level of recurrence does not systematically depend on the sample size.

The impact of the coupling on the atmospheric flow is likely most pronounced in regions where both $\overline{\tau}_w/\tau$ and $\overline{z}_0$ are large. This condition is best fulfilled in the Southern Ocean storm belt (Figs. 6 and 7). We consider zonally averaged quantities (which are more stable than the latitude-longitude field) because the number of test samples is fairly small. Two statistics of geopotential height at 500 hPa are investigated: the 30-day mean and the 2-15 day band-pass filtered variance. The levels of recurrence of the physically interesting signals are given in the following.

As can be seen in Fig. 8 the model troposphere responds to the presence of ocean waves by an increase in the 500 hPa geopotential height equatorward of 55°S ($p \geq 70\%$) and a decrease poleward of 55°S ($p \leq 20\%$). Thus, the climatological mean meridional pressure gradient is *enhanced* and shifted poleward in the WAM-ECHAM2 experiment. Consistently, the response in the band-pass (2-15 days) filtered 500 hPa geopotential variance reveals an interesting feature: poleward of 40°S the intensity, or frequency, of baroclinic disturbances is enhanced in the coupled model ($p \geq 75\%$) and equatorward of 40°S it is somewhat weakened ($p \leq 25\%$).

In the coupled experiment the meridional temperature gradient has changed by less than 0.5 K over the Southern Hemisphere at all atmospheric levels (not shown). The surface stress has increased by about 10% between 48°S and 60°S, and it has decreased by about 5% directly north and directly south of theses latitudes (not shown), consistent with the signal in geopotential height. The surface heat fluxes have not changed.

Figure 8

The zonally averaged difference in the geopotential height (in gpm) and the band-pass filtered (2 - 15 days) variance of geopotential height (in $(gpm)^2$) at 500 hPa between the coupled WAM-ECHAM2 experiment and the ECHAM2 control experiment (360-day mean).

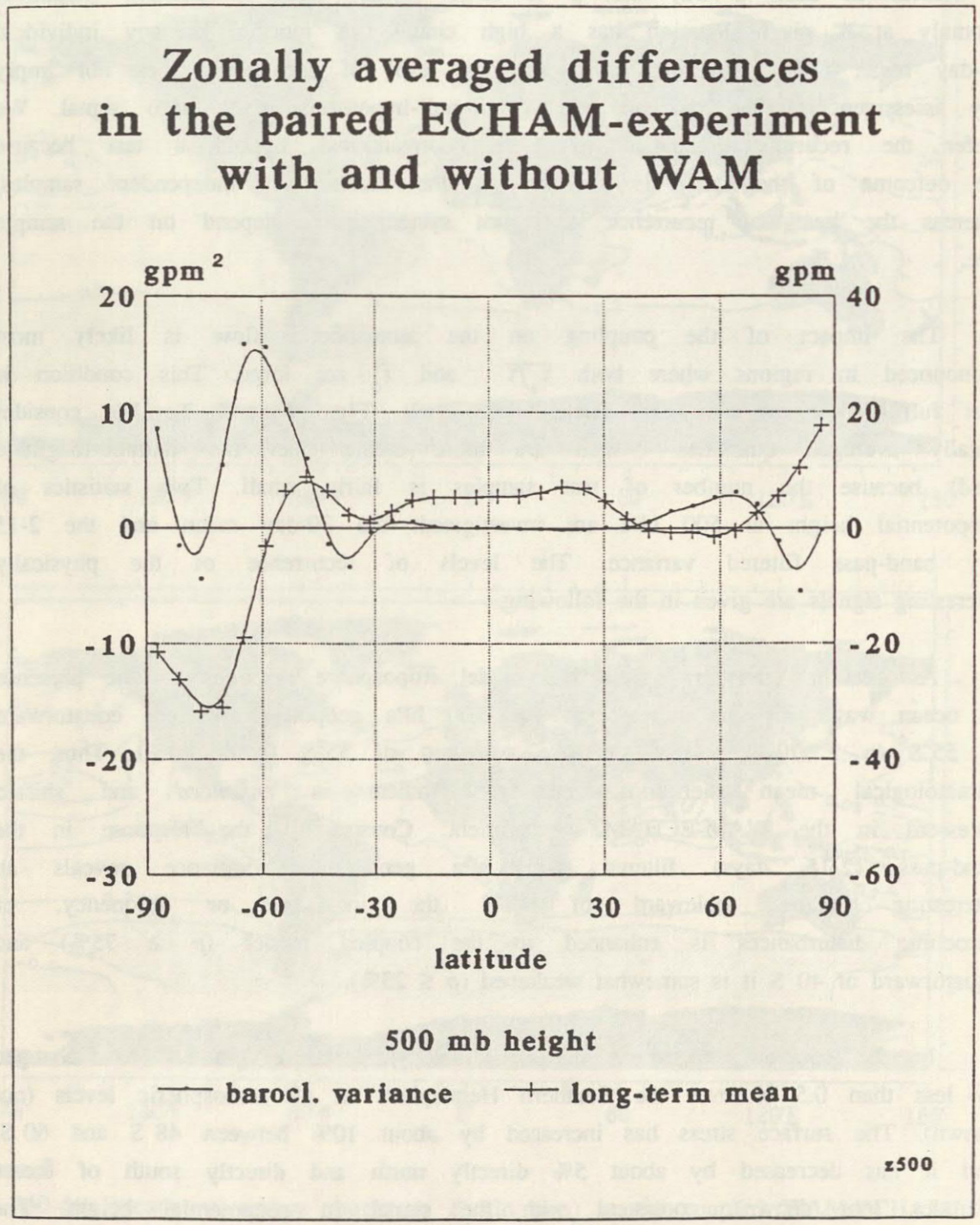

4. Summary and Discussion

We have, for the first time, coupled an ocean wave model (WAM) to a climate AGCM (ECHAM2) and have integrated it over an extended time. The wave model is forced by the surface wind stress whereas the waves modify the surface fluxes, depending on the stress ratio τ_w/τ. The coupled experiment produces a wave field climatology which is a consistent product of the simulated dynamics of the atmosphere and the wave field. The simulated wave heights are realistic. The simulated stress ratio and sea surface roughness seem reasonable. The coupling is weak in the mean in the Southern Hemisphere storm track and negligible everywhere else. The stress ratio exhibits a spatially and temporally highly variable pattern. This implies that the waves can have a significant impact on the evolution of individual storms.

The presence of the wave field in the coupled model yields a moderately strong but characteristic signal in the atmospheric circulation in the Southern Hemisphere: the mean meridional pressure gradient has steepened and the storm activity has shifted poleward and it has intensified south of 40°S, compared to the control run with the AGCM alone.

The zonally averaged time-mean enhancement of the sea surface roughness is extremely small. It is not likely that the mean planetary flow is directly affected by the modified surface stress and that the baroclinic variance changes as a result of this. It is interesting to compare the present experiment with that made by Ulbrich et al. (1991). They found that a zonally symmetric increase of the sea surface roughness (by a factor ten) in the Southern Hemisphere storm track is associated with weakened westerlies and with less, or weaker, storms. This is opposite to our findings.

An alternative explanation for the observed signal is what we refer to as the "storm-wave interaction" hypothesis. In this explanation it is important that the individual storms march over a sea surface with a spatially inhomogeneous roughness. Young wind sea is present in the equatorward area of a cyclone, where a "front" occurs with strong surface winds. Thus the equatorward side of a cyclone experiences a stronger surface stress than the poleward side. (The surface heat fluxes are not affected by the enhanced roughness, probably because the sea surface temperature is fixed in the experiments.) This patch of enhanced friction, which travels along with the cyclone, possibly forces the storm to move poleward. At the same time the frequency, or intensity, of the storms is enhanced.

The magnitude and the variability of the wind are too low in an AGCM with a coarse resolution like T21. This causes too low wave heights and reduces the possible impact of the coupling, as the wave-induced stress depends crucially on the strength and the variability of the wind field. The present experiment should therefore be regarded as a test, which shows that the coupling can indeed be significant.

One process which is not resolved in the T21 AGCM is the generation of subgrid-scale winds. There can be wave growth in a grid box due to small-scale wind systems, although the grid-box averaged wind is zero. This might be important in the convectively active areas in the tropics, where the atmospheric circulation is very sensitive to small changes in the surface heat fluxes (Miller et al., 1991).

The "storm-wave interaction" hypothesis has an interesting implication. We found the effect of the wave field on the atmospheric circulation to be of moderate relevance for the climatological mean circulation. The effect of the wave field on an individual storm, however, is significant as it seems to affect the path of a cyclone. We therefore hypothesize that wave growth is a process that is significant for weather forecasting.

ACKNOWLEDGEMENTS.

We thank Ulrich Schlese (Meteorological Institute of the University Hamburg) for his help in setting up the coupled model on the Cray 2 in Hamburg. Peter Janssen helped with advice, and Theo Opsteegh and Reindert Haarsma with constructive discussions. Heinz Günther (ECMWF) provided the global fields of wave height as forecast by the ECMWF. Ralph Weiße was bold enough to draw the fronts. Dierk Schriever made the color plots, and Doris Lewandowski and Marion Grunert prepared the diagrams. Grant Branstator critically read the manuscript. The experiments were performed during an eight month stay of SLW at the MPI in Hamburg; she thanks the MPI for its hospitality and for providing a very stimulating work environment. Financial support was given trough the EC (Grant EPOC 0003-C).

APPENDIX

Sensitivity of the AGCM to the minimum sea surface roughness

In this Appendix we examine the possible implications of using the unrealistically low minimum roughness length z_0 = 0.0001 mm.

Theory and measurements point to the presence of a minimum surface roughness. When the wind is weak the boundary layer flow is laminar. In this case the surface roughness scales with the thickness of the viscous boundary layer, which increases for decreasing wind speed. Instead of modeling the (small range of) viscous roughness lengths explicitly, one often imposes the minimum value which occurs at the transition from turbulent to viscous flow. Turbulence occurs at wind speeds above 3 - 8 m/s, depending on the atmospheric stability. The corresponding minimum roughness follows easily as 0.01 - 0.1 mm (using (1) and (2), with z = 10 m and assuming neutral conditions). Measurements also indicate that the roughness length has a minimum which lies between 0.01 mm and 0.1 mm.

Our choice of a minimum of only 0.0001 mm thus implies that we treat the low wind-speed cases incorrectly. We examine the z_0-distribution in our control experiment and in a standard ECHAM2 permanent-July control experiment (with a minimum roughness value of 0.15 mm). The distribution at two randomly chosen locations, one in midlatitudes and one in the tropics, is given in Fig. 9. In midlatitudes the roughness length in our control experiment rarely drops below 0.01 mm and in 20% of all cases it lies below 0.1 mm. We conclude that in midlatitudes a grossly unrealistic value is seldom used. In the tropics 40% of all values lie in our control experiment between 0.01 mm and 0.1 mm and 60% are below 0.01 mm. In the standard control experiment the minimum roughness value is always used in the tropics. The lowering of the minimum roughness value leads in the tropics to a decrease of the mean roughness length by an order of magnitude.

The change of the minimum roughness length from 0.15 mm to 0.0001 mm yields dramatic changes in our control run compared to the standard control run. Tropical convection is significantly reduced (rainfall over India had reduced by as much as 50%), and the heat fluxes in the warm water pool (the region around Indonesia and below the ITCZs in the eastern tropical Pacific and in the tropical Atlantic) are strongly weakened in our control run.

These dramatic changes are almost entirely related to modified heat fluxes, not to modified momentum fluxes. The rather high minimum of 0.15 mm in the standard control run was chosen to obtain sufficiently large heat fluxes in areas of low wind speeds like the tropics (Roeckner, personal communication). Therefore, the minimum value not only parameterizes the viscous boundary layer, but also the subgrid-scale winds.

Figure 9

The frequency distribution of the 12-hourly mean sea surface roughness z_0 (in mm) at two randomly chosen locations in two ECHAM2 control runs, one with minimum z_0 of 0.0001 mm and the other with a minumun z_0 of 0.15 mm (standard control run).

(a) 0° W, 37° S; a location in the Southern Hemisphere storm area

(b) 130° E, 8° N; a location in the West Pacific warm-water pool.

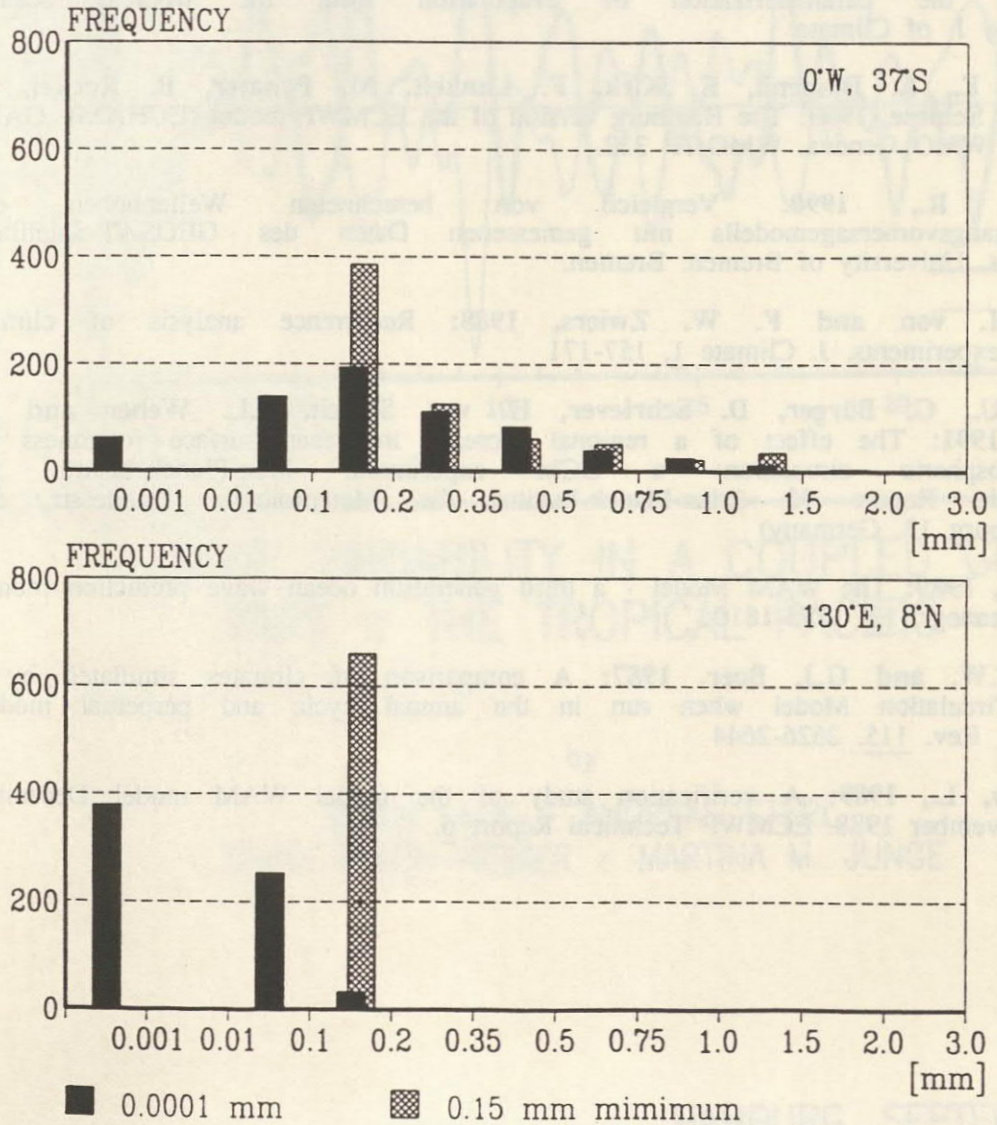

References

Charnock, H., 1955: Wind stress on a water surface. Quart.J.Roy.Meteor.Soc. 81, 639-640.

DeCosmo, J., 1991: Air-sea exchange of momentum, heat and water vapor over whitecap sea states. PhD-Thesis, University of Washington, 212 pp.

Hasselmann, K.H., 1990: Ocean circulation and climate change. Submitted to Tellus, also: MPI Report 58

Janssen, P.A.E.M., 1989: Wave-induced stress and the drag of air flow over sea waves. J. Phys. Oceanogr. 19, 745-754.

Janssen, P.A.E.M., P. Lionello and L. Zambresky, 1989: On the interaction of wind and waves. Phil. Trans. R. Soc. London A329, 289-301.

Maat, N., C. Kraan and W.A. Oost, 1991: The roughness of wind waves. Bound. Layer Met 54, 89-103.

Miles, J.W., 1957: On the generation of surface waves by shear flows. J.Fluid Mech. 3, 185-204.

Miller, M.J., A. Beljaars and T.M. Palmer, 1991: The sensitivity of the ECMWF model to the parameterization of evaporation from the tropical oceans. Accepted by J. of Climate

Roeckner, E., L. Dümenil, E. Kirk, F. Lunkeit, M. Ponater, B. Rockel, R. Sausen, U. Schlese, 1989: The Hamburg version of the ECMWF model (ECHAM). GARP Report 13, WMO Geneva, WMO/TP 332.

Romeiser, R., 1990: Vergleich von berechneten Wellenhöhen des WAM-Seegangsvorhersagemodells mit gemessenen Daten des GEOSAT-Satelliten. Sc.D. thesis, University of Bremen. Bremen.

Storch, H. von and F. W. Zwiers, 1988: Recurrence analysis of climate sensitivity experiments. J. Climate 1, 157-171

Ulbrich, U., G. Bürger, D. Schriever, H. von Storch, S.L. Weber and G. Schmitz, 1991: The effect of a regional increase in ocean surface roughness on the tropospheric circulation: a GCM experiment. Max-Planck-Institut für Meteorologie Report 70 (Max-Planck-Institut für Meteorologie, Bundesstr. 55, 2000 Hamburg 13, Germany)

WAMDIG, 1989: The WAM Model - a third generation ocean wave prediction model. J.Phys. Oceanogr. 18, 1775-1810.

Zwiers, F.W. and G.J. Boer, 1987: A comparison of climates simulated by a General Circulation Model when run in the annual cycle and perpetual modes. Mon. Wea. Rev. 115. 2626-2644

Zambresky, L., 1989: A verification study of the global WAM model December 1987 - November 1988. ECMWF Technical Report 6.